



## Investigation on transonic round convex-corner flows



Kung-Ming Chung<sup>a,\*</sup>, Po-Hsiung Chang<sup>b</sup>, Keh-Chin Chang<sup>b</sup>, Frank K. Lu<sup>c</sup>

<sup>a</sup> Aerospace Science and Technology Research Centre, National Cheng Kung University, Tainan, Taiwan

<sup>b</sup> Institute of Aeronautics and Astronautics, National Cheng Kung University, Tainan, Taiwan

<sup>c</sup> Aerodynamic Research Center, Department of Mechanical and Aerospace Engineering, The University of Texas at Arlington, Arlington, TX, USA

### ARTICLE INFO

#### Article history:

Received 29 October 2013

Received in revised form 12 May 2014

Accepted 13 May 2014

Available online 22 May 2014

#### Keywords:

Convex curvature

Shock

Boundary-layer separation

Pressure fluctuations

### ABSTRACT

Experiments were performed to investigate the flow of a transonic, turbulent boundary layer over regions of sharp and rounded convex surface curvature. The freestream Mach numbers were 0.64, 0.70, 0.83 and 0.89. Test models with three different radii of curvature from 13.7 to 41.7 times the upstream boundary-layer thickness were employed. The total turning angles were 13, 15 and 17°. The flow was found to be accelerated upstream of the curved region. The peak Mach number decreased with increasing radius of curvature for a given turning angle. In comparison with the sharp convex corner, a delay in the transition from subsonic to transonic expansion flows was observed. The shock structure, boundary-layer separation and peak fluctuating pressure were dependent on freestream Mach number, turning angle and radius of curvature.

© 2014 Elsevier Masson SAS. All rights reserved.

### 1. Introduction

Supersonic convex-corner flow is commonly known as Prandtl–Meyer expansion. In the transonic regime, a viscous-inviscid interaction is established around such an expansion. Ruban et al. [22] demonstrated that the displacement thickness near the corner is affected by the overlapping region that lies between the viscous sublayer and the main part of the laminar boundary layer. For a compressible, turbulent convex-corner flow, there are both upstream expansion and downstream compression near the corner apex. With a shock-induced, boundary-layer separation, an increase in peak Mach number results in upstream movement of the shock and downstream movement of reattachment, in other words, an increase in the separation zone [5]. Further, shock unsteadiness results in intense pressure fluctuations, in which the amplitude is roughly a constant value once the shock is sufficiently strong [4]. Similarity parameters have been proposed to characterize the flows, including peak Mach number, shock-induced, boundary-layer separation and peak pressure fluctuations [3,8,9]. In addition, the effect of tunnel background noise [10] and upstream disturbed boundary layer (normal blowing jet) [6,7] have been addressed. Intense discrete edgetones affect the interaction region and the amplitude of peak pressure fluctuations. A delay in

the transition from subsonic to transonic expansion flows with the upstream disturbed boundary layer is also observed. The fluctuating load in the case of shock-induced, boundary-layer separation is more sensitive to upstream disturbances [7].

Aircraft designs have employed flaps for takeoff and landing performance and ailerons for routine turning maneuver. Deflected control surfaces can also be employed in combination to provide variable-camber control during cruise flight [2]. In the previous studies [5,4,3,8–10,6,7], a sharp convex corner was adopted as an idealized configuration that models the deflection of a control surface. However, the presence of a short region of convex surface curvature would affect the flow structure such as upstream expansion, downstream compression, shock-induced, boundary-layer separation and flow unsteadiness and is therefore of fundamental interest. In the present study, surface pressure measurements and surface oil flow visualization were conducted to investigate the flow properties of compressible round convex-corner flows. A short region of convex surface curvature was presented and the total turning angles were the same as those of sharp convex corners. The effect of curvature is also addressed. Before discussing results of the present study, brief details of the experiment are outlined next.

### 2. Experimental program

#### 2.1. Transonic wind tunnel and test models

Experiments were conducted in the blowdown transonic wind tunnel at the Aerospace Science and Technology Research Center,

\* Corresponding author. Tel.: +886 62392811x210; fax: +886 62391915.

E-mail addresses: kmchung@mail.ncku.edu.tw (K.-M. Chung), kiby716@gmail.com (P.-H. Chang), kcchang@mail.ncku.edu.tw (K.-C. Chang), franklu@uta.edu (F.K. Lu).

### Nomenclature

$C_p$	pressure coefficient, $(p_w - p_\infty)/q$	$x$	coordinate along the surface of the corner, cm
$C_{\sigma_p}$	fluctuating pressure coefficient, $(\sigma_p - \sigma_{p_\infty})/q$	$x^*$	normalized streamwise distance, $x/\delta$
$M$	freestream Mach number	$X_i^*$	region of separated boundary layer
$M_1$	local Mach number upstream of shock	$\beta$	similarity parameter, $M^2\eta/\sqrt{1-M^2}$
$p_\infty, p_w$	mean surface static pressure	$\eta$	convex-corner angle, deg
$q$	freestream dynamic pressure	$\delta$	incoming boundary layer thickness, mm
$R$	radius of curvature, mm	$\sigma_p$	standard deviation of surface pressure

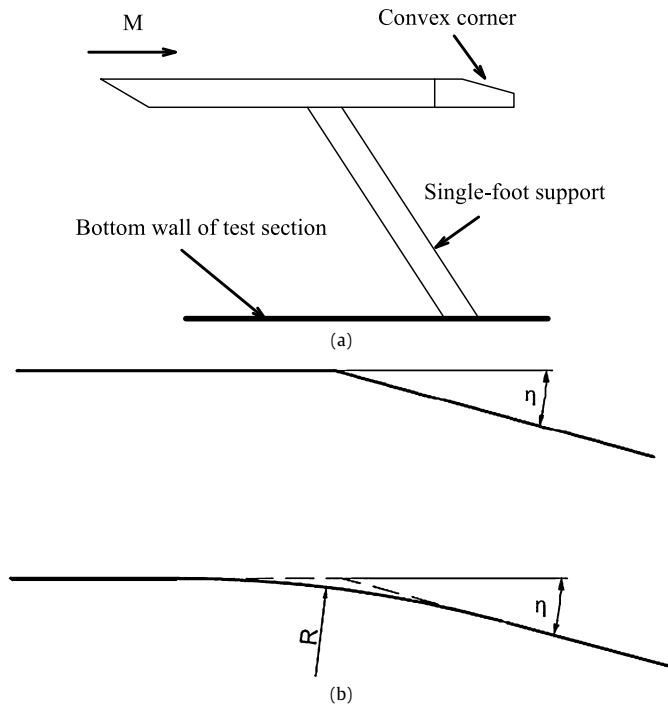


Fig. 1. Test configuration.

National Cheng Kung University. This facility includes compressors, a water cooling system, air dryers, storage tanks, and a tunnel. The constant-area test section is 600 mm × 600 mm in cross section and 1500 mm in length. In addition, the test section was assembled with solid sidewalls and perforated top/bottom walls in this study. The freestream Mach numbers  $M$  were 0.64, 0.70, 0.83 and  $0.89 \pm 0.01$ , and the unit Reynolds numbers ranged from 20.1 to 24.1 million per meter. The stagnation pressure  $p_0$  and temperature  $T_0$  were  $172 \pm 0.5$  kPa and ambient temperature, respectively.

The test model, which was supported by a single sting mounted on the floor of the test section, was comprised of a flat plate (150 mm wide × 450 mm long) and an interchangeable instrumentation plate with sharp or round corner, as shown in Fig. 1(a). For the test cases of sharp corner, as shown in Fig. 1(b), the instrumentation plate was 150 mm wide × 170 mm long and the convex corner was located 500 mm from the leading edge of the flat plate for a naturally-developed, turbulent boundary layer. The normalized velocity profiles for the undisturbed boundary layer at 25 mm upstream of the sharp convex corner appear to be full ( $n \approx 7$ –11 for the velocity power law), and the boundary-layer thickness  $\delta$  was estimated to be approximately 7 mm [4]. Nine round corner models were also fabricated with radii  $R = 100$  (R100), 200 (R200) and 300 (R300) mm ( $\delta/R = 0.024$ –0.073). Note that the region of convex surface curvature ranged from  $x^* = \pm 1.55$  to  $x^* = \pm 5.55$ . The deflection angle  $\eta$  ( $= 13, 15$  and  $17^\circ$ ) is given from the intersection of the tangential lines (virtual corner apex), as shown in

Fig. 1(b). One row of 19 pressure taps (6 mm apart) along the centerline of each plate was drilled perpendicularly to the test surface. To prevent cross flow from sidewall interference, side fences were installed at 75 mm on both sides of the taps.

### 2.2. Instrumentation and data acquisition system

For the surface pressure measurements, Kulite pressure transducers (XCS-093-25A, B screen) were employed and excited at 15.0 V by a power supply (Topward Electronic System, Model 6102). The pressure transducers had a nominal outer diameter of 2.36 mm and a pressure-sensitive element of 0.97 mm in diameter. The transducers were flush-mounted on the flat surface. Over the region of convex surface curvature, slight cavities formed in the pressure taps and these may cause a decrease in the amplitude of pressure fluctuations. Further, to improve the signal-to-noise ratio, external amplifiers (Ecreon Model E713, 12 channels) with a roll-off frequency of approximately 140 kHz, were also employed. A National Instruments (NI SCXI) system and the Labview program were employed to monitor the tests. The signals were acquired simultaneously and stored by NI-PXI high-speed data acquisition modules at a sampling rate of 200 ksamples/s/channel. In addition, to estimate the experimental uncertainty, experiments were conducted for the flat plate cases, without presence of a convex corner. Along the flat surface, the uncertainty values are 2.46% and 0.97% for the static pressure coefficient  $C_p$  and the surface pressure fluctuation coefficient  $\sigma_p/p_w$ , respectively. Moreover, surface oil-flow visualization was employed to visualize the surface flow pattern. A thin film of a mixture of titanium dioxide, oil, oleic acid and kerosene was applied on the surface of the instrumentation plate. For the attached flow, the surface streamlines over the whole span were straight and parallel to the incoming flow direction. With shock-induced, boundary-layer separation, the surface flow-field was not strictly two-dimensional. Accumulation of titanium dioxide was evident followed by the deflection of streamlines. The beginning of accumulation is taken as the separation position and the end of deflection is taken as the reattachment position. The region of separation and reattachment can be evaluated and compared with the surface pressure measurements.

## 3. Results and discussion

### 3.1. Wall pressure distributions

At lower Mach numbers and moderate convex-corner angles (sharp corner), the flow is purely subsonic [3]. Fig. 2 shows that the flow accelerates upstream of the corner (expansion) at  $M = 0.64$  and  $\eta = 13^\circ$ . The minimum surface pressure coefficient  $C_{p,min}$  is observed immediately downstream of the corner followed by subsonic compression, where  $x^*$  denotes the non-dimensional coordinate measured along the body surface from the corner apex. Flow expansion corresponds to the displacement effect of the boundary layer due to the overlapping region that lies between the viscous sublayer and main part of the boundary layer [22]. For

Download English Version:

<https://daneshyari.com/en/article/1718029>

Download Persian Version:

<https://daneshyari.com/article/1718029>

[Daneshyari.com](https://daneshyari.com)